Atmospheric and Topographic Effects Observed in Shadowed Pixels of Satellite Imagery

Yoshikazu Iikura

Faculty of Science and Technology, Hirosaki University
3 Bunkyo-cho, Hirosaki 036-8561 Japan
E-Mail : iikura@cc.hirosaki-u.ac.jp

ABSTRACT: With high sun elevation, the cosine law of solar incidence angle can be validated after the subtraction of offset component from satellite images. The offset component is mainly consisted of path radiance, which depends on target surface altitude in visible bands, in particular. With low sun elevaton, the irradiance from diffuse sky or adjacent slope might have significant effect. In this paper, these effects are quantitatively evaluated using shadowed pixels in actual satellite images (LANDSAT/TM).

1.Introduction

In satellite images over ruuged terrain, we can find several atmospheric and topographic effects which vary from one pixel to another. Though the solar incidence angle is the most significant topographical factor, there are some other minor factors such as[1),2),3)]

(1) the path radiance which depend on the altitude of the target pixels,
(2) the reduction of diffuse sky irradiation on the target pixels because the topography hides a part of sky hemisphere,
(3) the irradiation on the target pixel reflected by the adjacent slope.

When we deal with the satellite images with low sun elevation or hazy atmospheric conditions, careful attention should be paid to these effects though the precise correction seems difficult.

In this paper, we will evaluate these minor effects by using shadowed pixels of an actual satellite image (LANDSAT/TM). For this purpose, we prepare a digital elvation model which is consistent to the satellite image, and calculate some topographic parameters such as horizon[4)] and viewshed[5)] for each pixel as well as solar incidence angle. The satellite image is geometrically corrected to overlay these parameters.

2. Theoretical background

2.1 Modelling of satellite level radiance

Satellite level radiance(Ls) of target pixel (x,y) mainly consisits of reflected target irradiance(Io) and path radiance(Lp) as [2)]

$$Ls = Ts(z)R(x,y)Io + Lp(z) \quad (1)$$

where z is altitude, R is target reflectance, s is sensor scan angle, T s is transmittance from target to satellite.

Target irradiance (Io) is broken down into direct solar beam, diffuse sky irradiation Ed and irradiation from adjacent slope Ee as [1),3)]

$$Io = EoT\theta(z)\cos\beta + Ed + Ee \quad (2)$$

where $T\theta$ is transmittance from sun to target, θ is solar elevation angle, and β (solar incidence angle) is the angle between surface normal and the solar beam.

In the case of flat plane, there is no Ee and most parameters can be assumed constant. In the rugged terrain, however, not only solar incidence angle β but also path radiance and transmittance vary pixel by pixel. Irradiance from the diffuse sky and adjacent slope also depend on the local topography.

2.2 Correction of high sun elevation images

As Ed and Ee can be ignored for the satellite images with high sun elevation, topographical effects can be corrected using the cosine law of solar incident angle after the subtraction of offset component as

$$R(x,y)=(Ls-Lp)/EoTsT\theta\cos\beta \quad (3)$$

The parameters in eq.(3) are usually estimated by using radiative transfer code such as 6S[2] or Modtran[6]. However, there always remain some uncertainity in atmospheric conditions, in particular, aerosol concentration and characteristics. Conversion of the digital numbers into radiance is another error source.

In order to avoid these difficulties, Iikura et al.[7] have proposed the digital number based relative correction as

$$R(x,y) \sim (DN-a-b*z)/\cos\beta \quad (4)$$

where the dependence of path radiance is approximated by a linear function. This correction was based on the analysis of simulated data using 6S, which showed that the offset component decreases significantly in visible bands as the target altitude becomes higher, while it can be assumed constant in infrared bands. The analysis of shadowed pixels also supported the offset decrease in visible bands. In infrared bands, however, the DN in infrared bands have larger deviance than those expected from 6S simulation which assumes flat plane.

It is reasonable to think that the deviation of infrared bands is mainly caused by the irradiance of adjacent slope, because the used image was mainly occupied by the deciduous forest with high reflectance in infrared bands compared to visible bands.

3.Study Area and Data Base

In ordet to make our analysis clear, the Sirakami mountaneous region was selected as the study area, which is famous for its well preserved beech forest and covers 24 km by 21 km. From the vegetation map, the beech forest occupy about 70 % of the area as shown in Fig.1.

The Landsat TM image used for this study was aquired on November 2, 1998 (Path 108/ Row32). The study area is extracted and orthorectified to the UTM coordinate system (Zone 54) by using the carfully selected ground control points. The size of the image is 800 lines and 700 pixels with 30m resolution. Sun elevation angle (θ) is 32 degree and its azimuth angle (A) is 127 degree from the north. Figure 2 shows Band 5 image, which is used for the analysiis of adjacent slope effect.

Japan Geographycal Survey has published digital elevation model with latitude and longitude coordinate system with about 50m spatial resolution. We have transformed the DEM into UTM coordinate system as the satellite image. The bilinear interpolation is used for resampling.

4. Direct solar radiation

The direct solar radiation is propotional to the cosine of solar incidence angle β given as

$$\cos\beta = \sin\theta\cos e + \cos\theta\sin e\cos(\phi - A) \quad (5)$$

Fig.1 Beech forest area in Sirakami mountaneous region

Fig.2 Landsat TM image (Band 5) used in this study

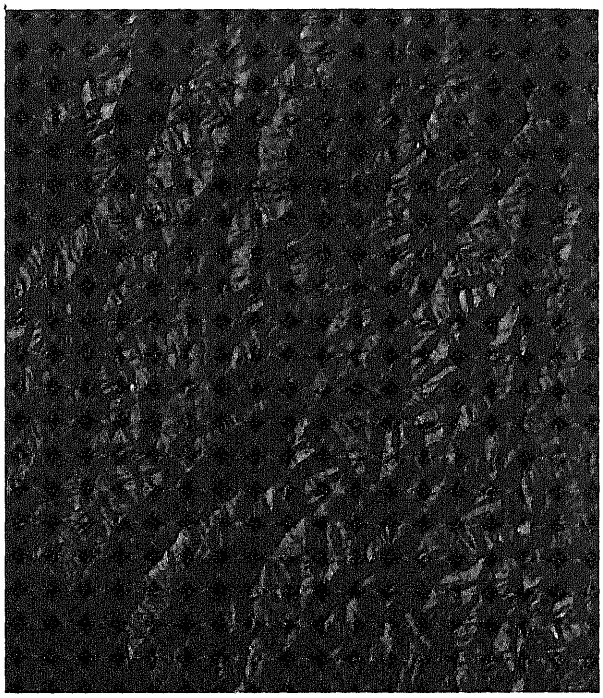

Fig.3 Direct solar radiation image calculated from the DEM

where e is slope angle and A is slope azimuth, which are calculated from the DEM. The cosβ is shown in Fig.3.

We can note the similarity between the satellite image and cosβ image. Their spatial correlation without displacement (δ =0)[8] is 0.74 as shown in Table 1. As the correlation for displaced satellite images, the accuracy of the geometrical correction is considered as within one pixel. It is also noted that Band 5 has higher correlation than visible bands because it is less atmosphecally influenced.

5. Extraction of shadowed region

There are two type of shadowed pixels, the one is self shadowed and the other is cast shadowed. The self shadowed pixel has negative cosβ, while the cast shadowed pixel has the higher horizon angle to the sun direction than theelevation angle of the sun.

Table 1 Change of correlation with displacement of the satellite image

δ	-2	-1	0	1	2
-2	0.34	0.46	0.58	0.66	0.68
-1	0.46	0.58	0.68	0.72	0.70
0	0.57	0.67	0.74	0.72	0.64
1	0.63	0.70	0.71	0.65	0.54
2	0.64	0.67	0.63	0.54	0.43

In one dimentional case, Dozier et al.[4] developed an efficient algorithm for the horizon computation. This algorithm has been extended to the two dimensional case by use of rotation and interpolation of the DEM[9].

Taking the ambiguity in the DEM and these calculation into consideration, we selected the the pixels of which cos β is less than -0.2 and of which horizon angle is less than 35degree. In Fig.4, the relationship between target altitude and digital number of the selected pixels are drawn. The DN of Band 1 decrease as the altitude becomes higher. On the other hand, there is no clear trend in Band 5 and it has large deviation.

6. Irradiance from the adjacent slope

The radiance recieved by the point M and coming from point P as shown in Fig.5 can be written as[1]

$$L_{MP}=(L_P dS_M \cos T_M \, dS_P \cos T_P)/r_{MP}^2 \qquad 6)$$

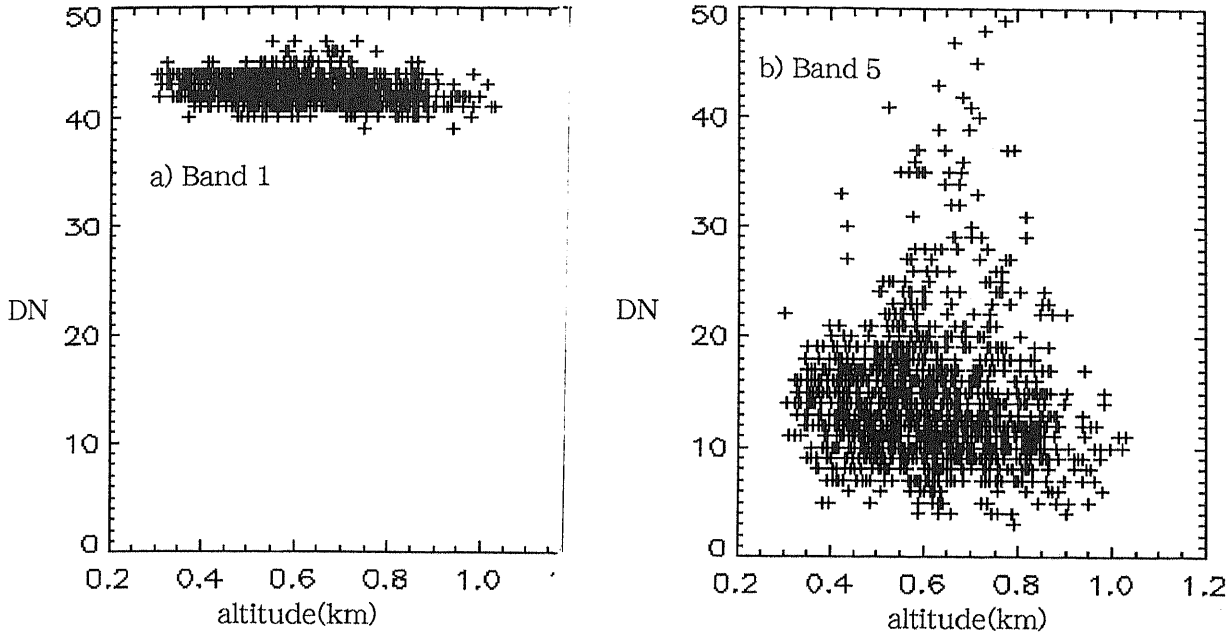

Fig.4 Relationship between DN and target altitude of shadowed pixels

where dS_M and dS_P are the areas of pixels M and P respectively, T_M and T_P are the angles between the normal to the ground and the line MP, L_P is the luminance of P, r_{MP} is the distance between M and P.

Though absolute value of Lp is not determined, it is natural to assume that Lp is propotional to the DN of pixel M. Then the total irradiance recieved by point M is relatively expressed as

$$E_M \sim \sum_P DN_P \cos T_M \, dS_P \cos T_P)/r_{MP}^2 \quad 7)$$

We call this adjacent slope factor. The sum must include the pixels which are oriented towards M and not hidden from pixel M, that is , the calculation of viewshed for each pixels is required.

As the viewshed calculation is time expensive, the approximate method has been usually applied to the actual satellite images[2),6),13)], which ignore the distance and radiation of adjacent slope.

Recently, fast algorithms for viewshed generation have been presented[10),11),12)]. Wang et al. applied their algorithm to the actual satellite images[3)], but they assumedthe homogenius

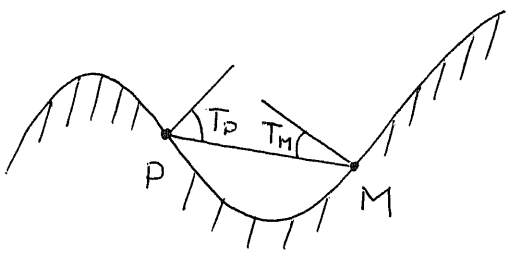

Fig.5 Geometrical consideration of the possible reflections from adjacent slopes

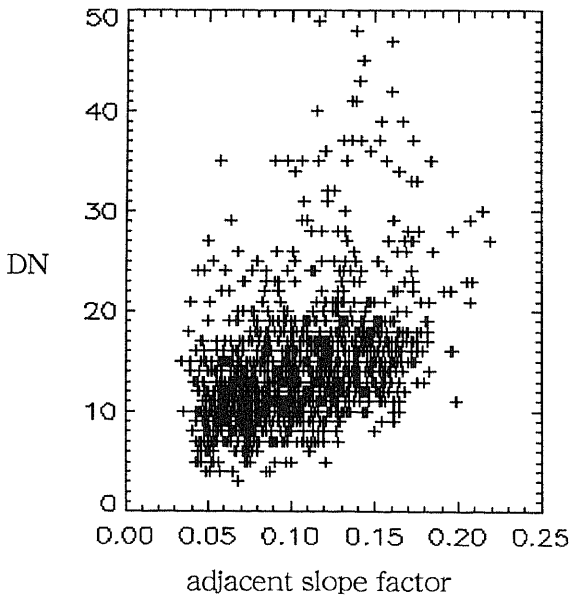

Fig.6 Relationship between adjacent effect factors and DN of shadowed pixels

surface. We apply the exact method with inhomogeneous surface expressed in Eq.7) to the selected shadowed pixels. Figure 6 shows the relationship between the DN of Band 5 and adjacent factors.It is seen that theshadowed pixels are effected by the irradiance from the adjacent slopes.

7. Conclusion

By using the shadowed pixels of the actual satellite image, we have evaluated the dependensy of path radiance in visible band and the irradiation from the adjacent slopes in infrared bands.

I will analyze irradiance from diffuse sky in visible band. Inaddition, these results should be analyzed statistically to develop the effective correction algorithm for the satellite image even with low solar elevation.

References

1) C.Proy, D.Tanre and Y.Deschamps : Evaluation of topographic effects in remotely sensed data, Remote Sensing of Environment, Vol.30, pp.21-32.,1989.

2) S.Sandmeier and K.Itten : A physically-based model to correct atmospheric and illumination effects in optical satellite data of rugged terrain, IEEE Trans. on Geoscience and Remote Sensing, Vol.35, No.3, pp.708-717, 1997.

3) J.Wang, K.White and G.J.Robinson : Estimating surface net solar radiation by use of Landsat-5 TM and digital elevation models, Int. J. Remote Sensing, Vol.21, pp.31-43.,2000.

4) J.F.Dozier et al. : A faster solution to the horizon problems, Computer & Geosciences, Vol.7, pp.145-151, 1981

5) P.Yoeli : The making of intervisibility maps with computer and plotter, Cartographuca, Vol.22, pp.88-103, 1985

6) R. Richter,Correction of atmospheric and topographic effects for high spatial resolution satellite imagery, Int. J. Remote Sensing, Vol.18, pp.1099-1111, 1997.

7) Y. Iikura and R.Yokoyama : Correction of atmospheric and topographic effects on Landsat TM imagery, J. of Remote Sensing Society of Japan, Vol.19, pp.2-16, 1999. (in Japanese)

8) Y. Iikura and R.Yokoyama : Determination of GCPs of Satellite Imagery using digital elevation mode, J. of Japan Society of Photogrammetry and RemoteSensing, Vol.37, No.6, pp.28-32, 1998. (in Japanese)

9) Y. Iikura : Interpolation of grid-based digital elevation models for fast horizon computation, Theory and Applications of GIS, Vol.8,No.2, pp.1-8, 2000.(in Japanese)

10) J.Wang, G.J.Robinson, K.White: A fast solution for computation local viewshed from gridded digital elevation models, Photogrammetric Engineering and Remote Sensing, 62, pp.1157-1164, 1996

11) J.Wang, G.J.Robinson, K.White: Generating viewsheds without using sightlines, Photogrammetric Engineering and Remote Sensing, 66, pp.87-90,2000

12) Y. Iikura : Systematic determination of invisible area using covering plane, Theory and Applications of GIS, Vol.8,No1, pp.39-46, 2000.(in Japanese)

13) J.F.Dozier, J.Frew : Rapid calculation of terrain parameters for radiation modelling from digital elevation data, IEEE Trans. on Geosciences and Remote Sensing, GE-28, pp.963-969,1990